JOURNAL OF CATALYSIS **87**, 292–304 (1984)

Surface Phases in Sulfided Ni–Mo/Al_2O_3 Catalysts

J. BACHELIER, M. J. TILLIETTE, J. C. DUCHET, AND D. CORNET

Structure et Réactivité d'Espèces Adsorbées (ERA 824), I.S.M.R.A., Université de Caen, 14032 Caen Cédex, France

Received July 20, 1982; revised December 12, 1983

The promoting action of nickel on sulfided Mo catalysts has been examined on two series of thiophene-sulfided Ni–Mo/Al_2O_3 catalysts with constant Mo content (7 and 16% MoO_3, respectively) and variable Ni concentration. The catalysts are characterized by their activity for thiophene HDS, by the fraction of Ni or Mo which can be extracted in an acidic or basic medium, and by their sulfur content. Comparison with "one-component" Ni/Al_2O_3 and Mo/Al_2O_3 catalysts shows that the dissolution of molybdenum is unaffected by the presence of nickel; by contrast, molybdenum lowers the non-extractable fraction of nickel, and thus partially hampers the migration of the promoter ions into the alumina matrix. The changes in the catalytic activity are discussed according to the amount of "free" (extractable) nickel Ni_F: three different roles of nickel are found and related to the nature of the surface phases. In the main promotion range of the first series ($0.1 < Ni_F/Mo < 0.6$), the results are consistent with increasing formation of a "Ni–Mo–S" phase which consists of small Mo entities associating almost two promoter atoms to three molybdenum atoms. For the high-Mo series, interaction between the Mo units leads to a different Ni–Mo–S association in larger patches, which limits at a lower Ni_F/Mo ratio the favorable effect of added nickel. Higher Ni content results for both series in bulk Ni_3S_2, unsuitable for further development in activity. At low Ni_F/Mo ratio, the catalyst structure is not elucidated.

INTRODUCTION

A large effort is currently being devoted to elucidating the nature of the Co(or Ni)–Mo(or W) active sulfided phase in alumina-supported hydrotreating catalysts. The objective is mainly to locate the Co(Ni) atoms in the promoted catalyst and thereby to explain the enhanced activity of the Mo(W)-based sample. Several descriptions of the structure, as derived from studies on both supported and unsupported systems, have been proposed:

(i) The monolayer model, based on the description by Schuit and Gates (*1*), of the Mo monolayer in registry with the alumina support in the calcined catalyst, supposes that surface oxygen atoms are replaced by sulfur, without modification of the molybdenum lattice; in this model, refined by Massoth (*2*) to account for steric effects arising from the O–S exchange, the promoter ions are thought to be located inside the alumina support. The other models ascribe to the starting Mo(W)/Al_2O_3 sulfided catalyst the structure of the MoS_2(WS_2) bulk sulfides.

(ii) The intercalation model, originally developed by Voorhoeve and Stuiver (*3*) in the case of unsupported Ni–W sulfide catalysts, attributes to the W sulfide, as bulk layered WS_2 crystallites, the ability to accommodate some intercalated Ni ions. Later, Farragher and Cossee (*4*) restricted the intercalation process to the edges of the crystals (pseudo-intercalation or decoration model). Such a description has been extended to the alumina-supported Co–Mo catalysts, implying that the sulfidation step destroys the Mo monolayer and converts it into MoS_2 crystallites, as demonstrated by de Beer *et al.* (*5*).

(iii) The contact synergy model proposed by Delmon (*6*) and co-workers assumes that a close contact between the separate MoS_2 and Co_9S_8 sulfide phases is responsible for the promoting effect.

(iv) The evidence for a "Co–Mo–S"

0021-9517/84 $3.00

phase presented by Topsøe and his colleagues affords an alternative structural description of both supported and unsupported Co-Mo catalysts (*7–9*). The active phase is regarded as a MoS_2-like structure, bearing Co atoms at the edges of the S–Mo–S slabs.

(v) Other models, based on semiconductor properties of the sulfides (*10*) or on surface segregation of the active components (*11*), have received much less attention.

At the present time the Co–Mo–S model of Topsøe *et al.* is strongly favored since a precise relationship could be established between HDS activity and the amount of active promoted phase for a wide range of Co–Mo catalysts, either unsupported (*12*) or dispersed on different supports (*8, 13, 14*). This could not be achieved with the previous hypotheses due to the lack of unambiguous specific physicochemical characterization of the active sulfide phase; moreover, the occurrence of promoter ions in different species on alumina-supported catalysts (surface spinel, bulk sulfide or some other specific combination) increases the complexity of the studies.

These obstacles have been overcome by Topsøe and co-workers, mainly by means of *in situ* Mössbauer spectroscopy and EXAFS. Their extensive researches lead to the description of a Co–Mo–S phase, several features of which are inconsistent with the previously proposed structural models. For instance, the Co atoms of both supported and unsupported Co–Mo catalysts show specific Mössbauer parameters (*9*) clearly distinguishable from those encountered for Co located in the alumina lattice and from other Co phases such as the Co_9S_8 sulfide. These observations are not consistent with the monolayer and contact synergy models.

Furthermore, in typical Co–Mo/Al_2O_3 catalysts molybdenum is thought to be highly dispersed as very small MoS_2-like domains in a two-dimensional state (*15, 16*). Such a structure does not allow cobalt intercalation (or pseudo-intercalation) which requires stacking of S–Mo–S sheets. Three-dimensional MoS_2 is observed on aged alumina-supported and also on unsupported catalysts (*17*). Thus, it now appears that the promoting effect in Co–Mo catalysts is related to the proposed Co–Mo–S phase.

Up to now Mössbauer spectroscopy has revealed the presence of a Co–Mo–S type phase also in Co–W/Al_2O_3 and Fe–Mo/Al_2O_3 catalysts, so that the proposed structure may be a general feature in hydrotreating catalysts. In this case Ni-promoted catalysts would also be expected to be described similarly, although spectroscopic evidence of a Ni–Mo–S phase is missing.

In the present studies, our aim is to characterize the active phase of sulfided Ni–Mo/Al_2O_3 catalysts by means of combined HDS activity measurements, chemical dissolution of the transition elements, and sulfur content determination. The results will be discussed by comparison with the "one-component" Ni/Al_2O_3 and Mo/Al_2O_3 previously studied (*18, 19*).

Since nickel extraction has proved to be an efficient way to measure the spinel fraction in Ni/Al_2O_3 catalysts (*20*), the technique will be used in order to quantify the active promoter ions. The relevance of the models and especially the possible occurrence of a Ni–Mo–S phase will be discussed with respect to the structure–activity relationship, further supported by our recent chemisorption results showing an enhanced activity of vacancies rather than an increase in their concentration on a promoted Ni–Mo catalyst (*21*). The Ni–Mo/Al_2O_3 catalysts under investigation differ by their Ni/Mo ratio which has been varied on two Mo-based catalysts with low and high loadings; an industrial catalyst is also included in the second series. In addition, the influence of the calcination temperature of the oxidic precursor has been studied on some samples.

EXPERIMENTAL

Catalysts

The Ni–Mo/Al_2O_3 catalysts containing

6.9 or 15.7 wt% MoO_3 are those previously used for oxygen and carbon monoxide chemisorption measurements (*21*).

The two series, denoted, respectively, as Mo-7–Ni-*x* ($0.4 < x < 4\%$ NiO) and Mo-16–Ni-*y* ($0.5 < y < 8.3\%$ NiO), undergo a final calcination at 500°C for 1 h. For a third series (Mo-16–Ni-4-*T*) containing 15.7% MoO_3 and 4% NiO, the final calcination temperature *T* has been varied from 350 to 550°C. In addition, *T* was raised to 700°C for the Mo-7–Ni-4 sample.

In all experiments, the sample of catalyst which is introduced in the reactor is recalcined for 2 h at a temperature corresponding to its preparation.

Catalytic Activity Measurements

According to a procedure already described (*19, 21*) the catalyst is stabilized without presulfiding by a thiophene–H_2 (1:12) mixture in a flow apparatus operating at 420°C and atmospheric pressure, and is kept for 24 h on stream before the HDS reaction products are analyzed chromatographically. The measurement of the HDS rate (r_{HDS}) at low conversion is then supplemented by measuring the rate of propene hydrogenation (r_{Hyd}).

Nickel and Molybdenum Extractions

The amounts of nickel and molybdenum that can be chemically extracted from Ni–Mo/Al_2O_3 catalysts have been determined at room temperature from two aliquots of the same sample: one is poured into 12 *N* hydrochloric acid to dissolve nickel and the other stands in a 12 *N* ammonium hydroxide solution to extract molybdenum. In case of oxidic samples, the selective dissolutions are completed in 24 h in both acidic and basic media. The sulfided catalysts are taken from the reactor after oxygen chemisorption at 60°C. Nickel extraction lasts for 24 h while the maximum molybdenum solubilization needs 7 days. In that case, the amount of molybdenum removed from the sulfided catalysts has also been determined after 24 h standing in ammonia. The metal contents of the solutions are measured by atomic absorption spectrometry.

Sulfur Analysis

The sulfur content of the catalysts is determined on samples which have been collected after oxygen uptake measurement. Thus, according to the chemisorption procedure (*21*), the sulfided catalyst is swept by a flow of argon for 2 h at 420°C. This purge ensures desorption of sulfur compounds resulting from the thiophene HDS reaction.

The sample is then collected from the reactor under nitrogen and transferred to a microanalytical combustion apparatus. A small addition of V_2O_5 prevents sulfation of the alumina during S analysis. The % S values reported here are corrected for a slight sulfidation of the support, determined from a blank experiment. They are given with an uncertainty of ±0.2%.

RESULTS

The characterization data for the Ni–Mo/Al_2O_3 catalysts are collected in Table 1.

Metal Extractions

As for one-component catalysts, chemical attack of the Ni–Mo samples according to the procedure described in the experimental section does not extract the total amount of the metals deposited on the alumina support.

Results for the Mo-7–Ni-*x* series are plotted in Fig. 1 versus Ni content in the solid. We first notice that molybdenum solubilization in ammonia remains unaffected in the presence of nickel, either in the oxidic or the sulfided form: 67% of the oxidic molybdenum is transferred to the solution and a larger fraction (87%) can be ultimately removed in 7 days from the sulfided sample. These results correspond to those already reported for low concentration Mo/Al_2O_3 catalysts (*19*). The solubility rate of the sulfided molybdenum remains high in the presence of promoter as shown by the small differences between extractions performed

TABLE 1

Characterization of Ni–Mo/Al$_2$O$_3$ Catalysts

Catalyst				Activities			10^3 Extractable metal (g · g^{-1})					10^4 N_S (mol S g^{-1})
Symbol	NiO (wt%)	Ni/Mo total	At. active[b]	10^3 r_{HDS} (mol h^{-1} g^{-1})	10^3 r_{Hyd} (mol h^{-1} g^{-1})	Selectivity r_{Hyd}/r_{HDS}	Nickel		Molybdenum			
							Oxidic	Sulfided	Oxidic	Sulfided		
										24 h	7 days	
Mo-7(6.9% MoO$_3$)				2.56	3.40	1.33			33.0	33.8	40.6	5.94
Mo-7–Ni-0.4	0.37	0.10	0.09	2.96	3.90	1.32	1.5	1.6	31.5	33.9	39.3	6.75
Mo-7–Ni-0.6	0.61	0.17	0.14	3.23	3.77	1.17	2.3	2.6	31.1	34.4	39.9	6.94
Mo-7–Ni-1.2	1.20	0.33	0.31	6.06	5.27	0.87	5.4	5.8	30.1	35.5	41.3	7.47
Mo-7–Ni-1.6	1.62	0.44	0.44	8.70	7.29	0.84	6.5	8.2	32.0	34.9	39.9	7.94
Mo-7–Ni-2	1.99	0.54	0.53	10.31	8.46	0.82	7.8	10.0	31.5	35.9	42.2	8.19
Mo-7–Ni-2.2	2.24	0.61	0.61	10.74	9.26	0.86	9.2	11.4	29.9	34.8	41.4	8.36
Mo-7–Ni-2.7	2.71	0.74	0.78	10.98	9.12	0.83	10.3	13.9	30.2	32.2	39.5	8.78
Mo-7–Ni-3.2	3.21	0.88	0.96	10.96	9.25	0.84	13.3	18.0	31.4	32.9	39.9	9.19
Mo-7–Ni-4	3.96	1.08	1.25	10.97	9.23	0.84	18.7	23.3	30.6	32.2	42.3	9.66
Mo-7–Ni-4–700	3.96	1.08	0.32	5.51	6.03	1.09	4.5	5.9	30.0	35.3	38.5	7.50
Mo-16(15.7% MoO$_3$)				5.78	10.00	1.73			64.3	43.6		14.5
Mo-16–Ni-0.7	0.7	0.09	0.04	7.11	9.88	1.39	1.9	2.2	62.6	50.1		15.0
Mo-16–Ni-1.2	1.16	0.14	0.07	9.52	10.71	1.13	3.6	4.1	60.7	49.4	73.5	14.8
Mo-16–Ni-4.3	4.29	0.53	0.36	31.03	16.40	0.53	15.0	19.2	63.5	49.5		19.4
Mo-16–Ni-8.3	8.32	1.04	0.85	28.02	15.56	0.56	37.0	45.6	58.5	48.8	80	22.9
HR346(14% MoO$_3$)	3.47	0.48	0.29	31.70	17.37	0.55	10.5	13.5	54.7	45.2	71.1	17.4
Mo-16–Ni-4.3 *T*.350[a]	4.29	0.53	0.48	26.14			27.2	25.7	64.5	46.7		
Mo-16–Ni-4.3 *T*.400	4.29	0.53	0.45	27.41			23.0	23.9	62.2	46.0		
Mo-16–Ni-4.3 *T*.450	4.29	0.53	0.42	30.44			20.5	22.5	62.0	42.7		
Mo-16–Ni-4.3 *T*.550	4.29	0.53	0.23	28.32			10.5	12.2	63.3	44.6		

[a] Calcination temperature *T*.

[b] $Ni_F/Mo_A \cdot Mo_A = (Mo_{total} - 1.7 \times 10^{-4})$.

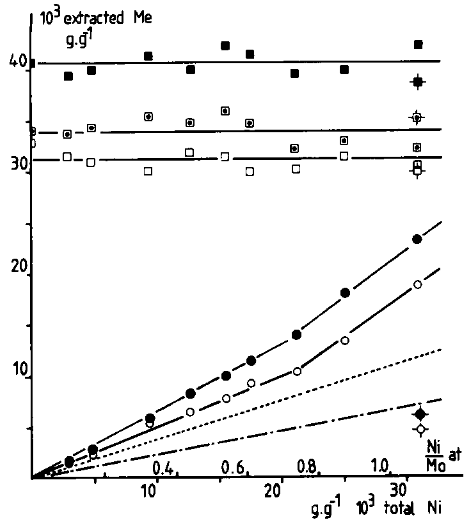

FIG. 1. Extraction of molybdenum and nickel from Ni–Mo/Al_2O_3 (Mo-7–Ni-x) catalysts as a function of the Ni content. Mo-7–Ni-x catalysts: extracted Mo, oxidic □; sulfided, extracted for 24 h ▣ and 7 days ■; extracted Ni, oxidic ○; sulfided ●. Mo-7–Ni-4 calcined at 700°C: extracted Mo, -□-, -▣-, -■-; extracted Ni, -○-, -●-. Ni/Al_2O_3 catalysts: extracted Ni, oxidic — · —; sulfided - - - (Ref. (*18*)).

for 24 h or 7 days. Second, nickel extractions by acidic attack of both calcined and sulfided samples increase with the Ni content, but the plot is split up into two linear parts. In the case of oxidic samples, up to Ni/Mo = 0.7, only 50% of the nickel can be removed, while almost the whole of the nickel added beyond this loading is extracted. Sulfided catalysts behave essentially in the same manner, with the same breaking point at Ni/Mo $\simeq$ 0.7, but the slope of the first section corresponds to a 68% extraction of the nickel added; the slope then again increases and approaches 1, indicating that a further nickel content can be totally solubilized. Referring to the one-component Ni/Al_2O_3 catalyst (*18*), it can be seen that nickel extractions are favored in the presence of molybdenum. Since the unextractable nickel was previously identified as surface spinel (*20*) incorporated into the alumina support, it is clear that free nickel (Ni_F) is present in larger amounts in Ni–Mo than in Ni/Al_2O_3 catalysts.

With respect to the Mo-16–Ni-y catalysts, with high Mo content, in spite of an incomplete series (Table 1), one can see in Fig. 2 that they follow the same trend as the previous series. The presence of nickel has still no influence on the labile fraction of molybdenum: ammonia removes about $\frac{2}{3}$ of the total Mo from the oxidic samples, and a larger fraction from the sulfided form. Even the solubility rate of the sulfided molybdenum is not significantly affected, since an almost constant amount (43 to 50 mg g^{-1}) is released after a 24-h standard attack. On those catalysts, the fraction of nickel which can be acid-extracted increases with Ni loading, and the highly loaded Mo-16–Ni-8.3 loses more nickel than the other samples, in both calcined and sulfided states. However, the small number of catalysts does not allow us to distinguish any clear limit. Nevertheless, these results confirm that molybdenum hampers nickel ion migration into the support.

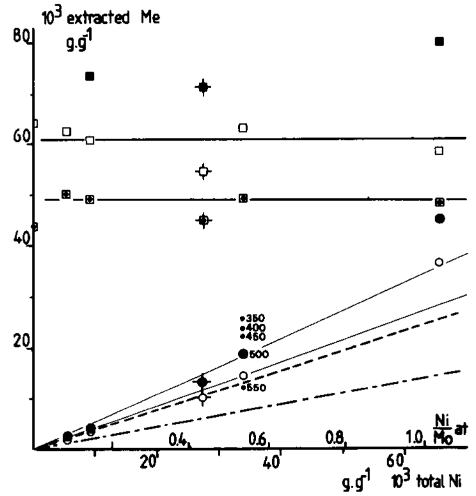

FIG. 2. Extraction of molybdenum and nickel from Ni–Mo/Al_2O_3 (Mo-16–Ni-y) catalysts as a function of the Ni content. Mo-16–Ni-y catalysts: extracted Mo, oxidic □; sulfided, extracted for 24 h ▣ and 7 days ■; extracted Ni, oxidic ○; sulfided ●. HR.346 catalyst: extracted Mo, -□-, -▣-, -■-. Mo-16–Ni-4.3-*T* catalysts: extracted Ni, sulfided ●. Ni/Al_2O_3 catalysts: extracted Ni, oxidic — · —; sulfided - - - (Ref. (*18*)).

Catalytic Activity

Activity data of the two series of Ni–Mo/Al_2O_3 catalysts for thiophene HDS are presented in Table 1 (see also Fig. 1 in Ref. (*21*). The promoting effect of nickel ions is obvious and depends upon the Ni content: the first nickel ions are not effective promoters but a maximum in activity is found approximately at Ni/Mo = 0.6 in both series.

However, these raw data cannot be directly used to infer the Ni concentration in the promoted active phase since on a γ-alumina support, a fraction of the deposited metal ions is converted to ineffective species in the sulfide catalysts. Thus, the nature of Ni^{2+} ions in the spinel structure of $NiAl_2O_4$ make them totally inert in HDS; the active fraction corresponds to the free nickel atoms Ni_F, extractable by hydrochloric acid, and consequently easily quantified.

In case of molybdenum, active and inactive species are not distinguished according to their solubilization in ammonia, but both HDS activity and chemisorption on Mo/Al_2O_3 catalysts start at a threshold of about 3% MoO_3 (*19*); hence, it is of value to take in account the amount of active molybdenum, e.g., Mo_A (mol g^{-1}) = $Mo_{total} - 1.7 \times 10^{-4}$. For these reasons, the activity data shown in Fig. 3 are plotted against the Ni_F/Mo_A atomic ratio instead of Ni_{total}/Mo_{total} generally found in the literature.

For the Mo-7–Ni-x series, the promoting action starts at $Ni_F/Mo_A \simeq 0.1$ for both hydrogenolysis and hydrogenation reactions, indicating surprisingly that the very first "free" nickel (0.3×10^{-4} mol g^{-1}) practically does not affect the activity of the Mo-7/Al_2O_3 base catalyst. The phenomenon seems much less pronounced for the other series, and thus questionable. In fact, one can verify, using Ni_F instead of Ni/Mo as abscissae, that it is likely to occur to the same Ni_F extent in both series. As the nickel content rises, a large promotion range is then observed, reaching distinct maxima for the two types of catalysts at 0.6 and 0.35, respectively, while they were found at about similar ratios (0.6) when considering the bulk composition of the samples (*21*). Finally, beyond the maximum, the beneficial action of nickel ceases. Thus, the available promoter on the Ni–Mo/Al_2O_3 catalysts gives rise to three different promoting effects. This is also evidenced by the selectivity $S = r_{Hyd}/r_{HDS}$ for the set of low Mo samples: starting at the Mo-7 value ($S = 1.3$), S gradually decreases in the promotion range and finally stabilizes around 0.8. The final selectivity (0.5) for the high Mo series corresponds to that observed for the Ni/Al_2O_3 catalysts (*18*).

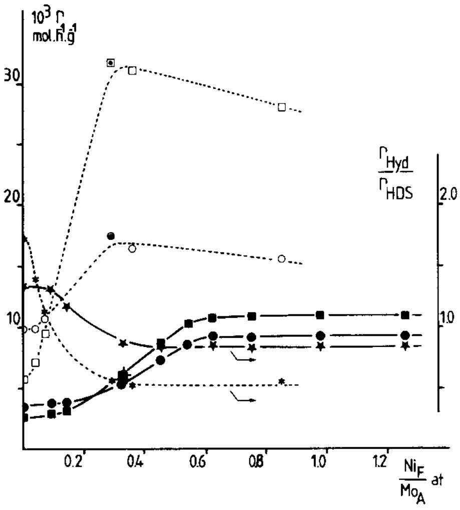

FIG. 3. HDS and hydrogenation activities of Ni–Mo/Al_2O_3 catalysts as a function of the corrected composition ratio Ni_F/Mo_A. Mo-7–Ni-x catalysts: ■ HDS, ● Hyd, ✱ selectivity; Mo-7–Ni-4 calcined at 700°C: ⊞, ⊕. Mo-16–Ni-y catalysts: □, ○, *; HR.346 catalyst: ▣, ◉, ✱.

The industrial catalyst HR 346 is close to the maximum catalytic efficiency of the promoted Mo-16–Ni-y samples.

Sulfur Content

The sulfur content expressed as N_S (mol S per g catalyst) for the thiophene-sulfided catalysts increases with Ni concentration (Table 1). As for the activity data, a corrected Ni/Mo ratio, relative to the only sulfid-

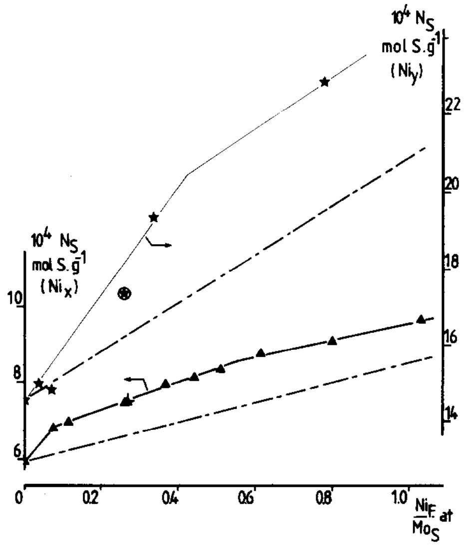

FIG. 4. Sulfur content N_S of Ni–Mo/Al_2O_3 catalysts as a function of the corrected composition ratio Ni_F/Mo_S. Mo-7–Ni-x catalysts: ▲. Mo-7–Ni-4 calcined at 700°C: -▲-. Mo-16–Ni-y catalysts: ★; HR.346 catalyst: ⊛. Theoretical N_S with Ni as Ni_3S_2 —·—·—.

able species is used as abscissa in Fig. 4 to show the evolution of N_S as a function of composition. It is assumed that nickel spinel does not sulfide, so that free nickel Ni_F has been taken into account. In the case of molybdenum, we have considered Mo_S (mol g^{-1}) = $Mo_{total} - 1 \times 10^{-4}$. The threshold for sulfided (10^{-4} mol Mo g^{-1}) was found previously in thiophene-sulfided Mo/Al_2O_3 catalysts (*19*); it appears lower than for activity (1.7×10^{-4}). The corresponding plot for the Mo-7–Ni-x set of samples again shows three linear sections with the same limits as for the activity data. From the slopes it can be deduced that the promoted catalysts gain one sulfur per free nickel atom added in the promotion range. This is more than would yield a simple addition of bulk nickel sulfide Ni_3S_2. However, the stoichiometry $\Delta N_S/\Delta Ni_F$ is found equal to 0.64 in the third range, beyond the maximum at $Ni_F/Mo_S \simeq 0.6$. By contrast, sulfur content increases very sharply at low Ni concentration.

Results are less consistent with respect to the second series Mo-16–Ni-y, due to lack of data. Nevertheless, the Ni–Mo catalysts appear to sulfide to a larger extent than the sum of their individual components (Fig. 4).

Influence of the Calcination Temperature

The second calcination step performed on the Mo/Al_2O_3 sample after nickel introduction greatly influences the properties of the promoted catalysts. Thus, the Mo-7–Ni-4 sample, calcined at 700°C for 2 h (Mo-7–Ni-4-700) instead of 500°C is characterized (Table 1) by a lower activity (Fig. 3), a lower sulfur content (Fig. 4), and lower chemisorption capacities (*18*) which all make it resemble the Mo-7–Ni-1.2 catalyst, calcined in the standard way at 500°C, but with lower total Ni content.

Examination of the extraction data further reveals that molybdenum solubilization is unaffected by the high-temperature treatment (Fig. 1). However, the Ni spinel fraction strongly increases. As a result, the Ni_F/Mo_A ratio is dramatically lowered from 1.2 to 0.3, this final value being close to that encountered in the Mo-7–Ni-1.2 catalyst normally treated at 500°C.

For the Mo-16–Ni-4 catalyst (Table 1) which, in the Mo-16–Ni-y series compares reasonably well with the industrial catalyst HR 346, the final calcination temperature has also been varied from 350 to 550°C. Again the main effect is a variation in amount of nickel extraction: Ni_F regularly decreases with increasing temperature, and more rapidly beyond 450°C (Fig. 2). However, this change is not connected with the catalytic activity which tends to go through a maximum between 450 and 500°C.

DISCUSSION

In typical mixed sulfide catalysts supported on alumina, the promoter ions are distributed in different phases which contribute at different levels to the overall activity of the sample. Among them, and extensively studied in the case of the Co–Mo/Al_2O_3 system, the spinel $CoAl_2O_4$ is recognized as inactive, and the bulk sulfide Co_9S_8 of moderate activity. Other phases are unlikely to occur on alumina-supported catalysts. From the investigations of Topsøe and co-workers (*9*), it is concluded that the main catalytic role is devoted to a "Co–Mo–S" phase. As already mentioned, analogs of this phase have been found in other mixed sulfide catalysts, so the results reported here for the Ni–Mo/Al_2O_3 samples will tend to be discussed in terms of this particular structural model.

The characterization data, activity and sulfur content of the Ni–Mo/Al_2O_3 catalysts studied here as a function of their nickel content have been considered on the basis of the effectively available nickel or molybdenum for the catalytic sulfide phase. This seems the right way to study the promoting effect according to the promoter concentration since, by using this new parameter, it is possible to make the Mo-7–Ni-4 catalyst, calcined at 700°C, fit on the regular curves established for the normal samples of the series.

Such a presentation of the results is based on the quantitative determination of the Ni and Mo species which participate in the active phase. In the case of nickel, this could be achieved by acid attack of the sulfided catalysts which could differentiate between free nickel Ni_F and surface spinel. For molybdenum, Mo_A is deduced from surface properties of the samples, namely HDS activity and chemisorption, instead of ammonia extraction which affects also the bulk atoms. In fact, molybdenum interacts much less strongly than nickel with the alumina, and readily rearranges on the support after basic attack (*19*).

When considering the Ni_F/Mo_A ratio, three promoter concentration ranges are observed in both series, for which the added nickel behaves differently with regard to the Mo/Al_2O_3 based catalyst. Second, for low and high loadings of the starting Mo/Al_2O_3 sample, the maximum promoting effect does not occur at the same Ni_F/Mo_A composition. Interpretation of the phenomena will include chemisorption results obtained on the same catalysts (*21*).

Effective Promotion Range

Wivel *et al.* (*8*) have shown that the distribution of the cobalt atoms between the different phases of a Co–Mo/Al_2O_3 catalyst depends on the promoter concentration. Cobalt aluminate is always present; the amount of Co–Mo–S phase increases in the Co/Mo promotion range and beyond it the Co_9S_8 sulfide predominates. Hence, with respect to the Ni–Mo/Al_2O_3 catalysts, the physicochemical characterizations obtained in the Ni/Mo promotion range (from the sulfur content reported here and the chemisorption results previously reported (*21*)) are expected to be representative of an analogous "Ni–Mo–S phase," since the nickel aluminate does not contribute to these. Results lead us to distinguish the two Ni–Mo series studied, in view of their different fits to the particular Co–Mo–S type structural model.

Low-Mo Concentration Ni–Mo/Al_2O_3 Catalysts: Possible Occurrence of a Ni–Mo–S phase

State of molybdenum. The nature of molybdenum in the Co–Mo–S type phase has been deduced by Clausen *et al.* from EXAFS studies (*15*), and completed by Topsøe in an ir investigation (*16*). They conclude that for a typical sulfided Co–Mo/Al_2O_3 (13.6% MoO_3) catalyst there is a highly dispersed two-dimensional MoS_2-like structure in small domains, which is similar to that encountered in Mo/Al_2O_3 samples. In respect to this structure, the cobalt atoms are most probably located at the edge sites of the MoS_2 slabs. The high degree of dispersion allows a large amount of promoter to be accommodated by molybdenum in the Co–Mo–S phase structure, in a ratio Co/Mo $\simeq 0.5$ at the maximum of the promoting effect.

Most of these features can be recognized in the Mo-7–Ni-*x* series. The same amount of molybdenum is solubilized in both promoted and unpromoted samples, so it is likely that the nature and dispersion of molybdenum remain unaffected by the presence of Ni atoms. Thus the model proposed for the sulfided Mo/Al_2O_3 catalysts (*19*) holds in the presence of promoter. We had pictured there a polythiomolybdate active phase, partially bound to the alumina. Mo entities have been characterized in the 3–10% MoO_3 (about half a monolayer) concentration range which are assumed to be of small and constant size, isolated from each other, as proposed for Co–Mo–S. Hence the state of molybdenum in the Mo-7–Ni-*x* catalysts agrees well with that proposed for a Co–Mo–S type phase, especially with respect to the high degree of dispersion, and one could easily regard the small Mo units as being similar to the two-dimensional MoS_2 slabs. However, in view of the incomplete dissolution of the sulfided molybdenum, we have suggested anchorage of the domains to the support by some Mo ions. It might be possible that such a bonding, which has not appeared in the Co–Mo–S studies, is due to the mild sulfidation of the catalysts by thiophene, since the fraction of free molybdenum increases upon more severe sulfiding (*19*).

State of nickel. When considering the state of the promoter atoms in the Mo-7–Ni-*x* catalysts, it is noteworthy that the free Ni_F nickel fraction is larger in Ni–Mo catalysts than in Ni/Al_2O_3 samples. This can be interpreted as ascribing to molybdenum a tendency to hold Ni ions during their diffusion process toward the alumina. This phenomenon is observed on both calcined and sulfided samples, so that the oxidic catalyst could be regarded, in agreement with the Topsøe work (*22*), as an active precursor of the sulfided phase. However, such an oxidic combination is not critical for the final formation of the active Co–Mo–S type phase in view of the similar sulfide phase found on carbon-supported samples, without any calcination step (*14*). The oxidic precursor seems specific to the alumina-supported catalysts.

The sulfur content determination also distinguishes nickel in the Ni–Mo couple from the Ni_3S_2 sulfide found in the Ni/Al_2O_3 catalysts. It argues in favor of Ni atoms losing their individuality, as happens for Co in the promoter–molybdenum association in the Co–Mo–S proposal.

Further information about the state of nickel can be inferred from the chemisorption of oxygen and carbon monoxide probe molecules by the Mo-7–Ni-*x* samples (*21*). The combined observation that gas uptake is proportional to the Ni content (as also found for the Ni/Al_2O_3 samples) and that it correlates with the HDS activity in the Ni/Mo promotion range suggests that active sites are introduced by nickel atoms themselves, or created by their association with the small molybdenum entities. In any case, the promoter is most probably located at surface sites, and among several possibilities the edges of the MoS_2 slabs (as proposed in the Co–Mo–S model) may very well be in line with our results. Accordingly, the large amount of nickel that the Mo phase can accommodate ($Ni_F/Mo_A \simeq 0.6$ at maximum) would confirm the very small size of the starting Mo units. If one cannot speak in terms of a definite phase in its classical sense, it should be mentioned that the constancy in the specifications of the Mo entities will result in a Ni–Mo–S phase with a definite stoichiometry. The proposed structure of the Mo-7–Ni-*x* catalysts is schematically pictured in Fig. 5.

High-Mo Concentration Ni–Mo/Al_2O_3 Catalysts: Deviation from the Co–Mo–S Type Model

For the Mo-16–Ni-*y* series, more concentrated in molybdenum, the nickel extraction data and the sulfur content lead us to consider the nickel atoms as being different in the promoted catalyst from those characterized in the Ni/Al_2O_3 samples. An association of nickel and molybdenum is likely to occur, as in the previous Ni–Mo series. However, some features differ in the two series, with the result that the properties of

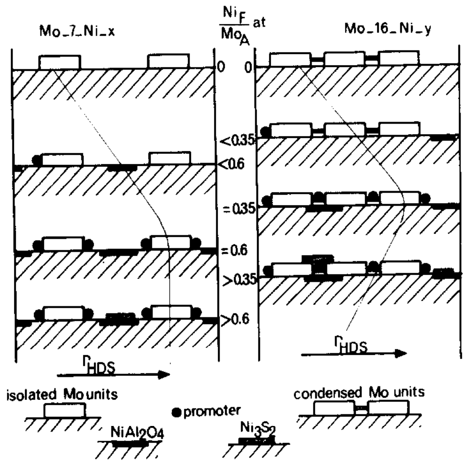

FIG. 5. Schematic proposed structures of the thiophene-sulfided Ni–Mo/Al_2O_3 catalysts.

Mo-16–Ni-*y* are not fully consistent with the description of the structure as being of the Co–Mo–S type.

Thus, the maximum promoting effect in the Mo-16–Ni-*y* series is found at a lower Ni_F/Mo_A value as compared to the other series (0.35 against 0.6, Fig. 2). This could be interpreted as meaning a change in particle size upon increasing Mo concentration, yielding some hidden surface positions for the Ni atoms. In fact, ESCA measurements performed on the same Mo and Ni–Mo samples do not detect any stacking of molybdenum upon increasing Mo content up to a monolayer, in both promoted and unpromoted catalysts (*23*). Hence the change in dispersion in the Mo-16–Ni-*y* series is likely to occur by enlargement of the Mo domains, still spread on the support in a two-dimensional state. This would lead to a lower fraction of surface present as edges, and, according to the Co–Mo–S type model, to a lower amount of promoter in the Ni–Mo–S phase.

However, this description of the Mo-16–Ni-*y* catalysts is not in line with the chemisorption results. It is found that, by contrast with the Mo-7–Ni-*x* series, the chemisorption capacity of those catalysts is not influenced by the amount of promoter in the Ni/Mo promotion range. This is not expected from the Co–Mo–S type model which, as discussed above, would affect the amount of edge sites, but not their accessibility.

The different properties of the high-Mo Ni–Mo/Al_2O_3 catalysts may originate from the different structure of the corresponding Mo-based sample. We have shown in a previous examination of sulfided Mo/Al_2O_3 catalysts (*19*), that upon increasing Mo content, the small Mo entities characterized in the range 3–10% MoO_3 do not remain isolated, but interact each other, probably at their edges. This condensed structure is likely to apply in promoted samples since the dissolution of molybdenum is unaffected by the presence of nickel. Therefore, in view of the proximity of the Mo entities on those catalysts, it cannot be excluded that the promoter atoms, still located at edge sites, are now shared between two Mo groupings as shown in Fig. 5. Thus the catalyst will accommodate at maximum less Ni per Mo atom in the condensed structure than in the isolated one and the Ni_F/Mo_A ratio will depend on the number of interacting units. Moreover, the interstitial positioning of nickel ions may suppress their chemisorption properties compared to the substitutional edge positions proposed in the Co–Mo–S type model. The possible consequences on the HDS sites will be discussed in the next section.

The Co–Mo–S model has been derived by Topsøe and co-workers from a Co–Mo/Al_2O_3 series based on a 13.6% MoO_3/Al_2O_3 catalyst. Therefore one may be surprised that our results for the Mo-16–Ni-*y* catalysts, with a comparable Mo content, are not fully explained by this particular model. Moreover, we find a maximum in activity at a Ni_F/Mo_A ratio well below that reported by Wivel *et al.* (*8*) for the Co engaged in the Co–MoS phase (0.35 against 0.5). It is possible that the cobalt and nickel atoms do not show exactly the same properties, and thus lead to somewhat different Co(Ni)–Mo–S phases. However, in view of the satisfactory explanation brought by the Co–Mo–S type phase to the lower Mo-content Mo-7–Ni-*x* catalysts, it seems that the nature of the promoter ions is not suspected. More likely, it should be remembered that our catalysts are activated under thiophene and not presulfided. In that sense, Clausen *et al.* (*15*) have shown that molybdenum is disordered in the calcined catalysts and reorganizes upon sulfiding. We suggest that reorganization leads to the specific Mo entities we have characterized for low Mo-content catalysts. From our results, the mild thiophene sulfidation would be able to create these entities at low Mo concentration, while they would be only preformed in the case of higher Mo content. Normal sulfidation would achieve the ordering of molybdenum in any case. Such an effect of presulfiding is supported by the O_2 chemisorption results reported by Burch and Collins (*24*). The presulfided 15% MoO_3 Ni–Mo/Al_2O_3 catalysts they have studied show an increase in O_2 consumption with increasing Ni content, whereas uptake is not influenced by the Ni concentration in the case of our thiophene-activated Mo-16–Ni-*y* samples. Finally, as shown by the Topsøe work (*17*), a three-dimensional state could be obtained in more severe sulfiding conditions.

Active Sites on Ni–Mo/Al_2O_3 Catalysts

With respect to the role of the promoter in the mixed sulfide catalysts, there is now agreement that the nature of the active sites is changed on going from unpromoted to promoted mixed sulfide catalysts. This conclusion is mainly supported by kinetic analysis of the HDS reaction on a series of cobalt-promoted molybdenum catalysts (*8*). It is fully in agreement with our chemisorption results (*21*) since they led us to conclude that the enhanced activity of a Ni–Mo catalyst arises from an activation of the thiophene adsorption sites rather than their multiplication. However, the exact role of the promoter atoms is not elucidated. Two very probable situations are discussed by Topsøe (*25*) in connection with the Co–Mo–S structure of the active phase, namely that the promoter either acts by itself in the HDS reaction or it creates active neighboring molybdenum atoms. In the case of the Mo-7–Ni-*x* catalysts, for which an analogous Ni–Mo–S phase seems to apply, the chemisorption data (*21*) cannot discriminate between these possibilities since the probe molecules which were used titrate vacancy sites whatever their origin. A more precise description of the active sites may be drawn in the case of the Mo-16–Ni-*y* catalysts: since those promoted catalysts are no more sensitive to chemisorption than the unpromoted Mo-based catalyst, it may be inferred that the active sites of the Ni–Mo catalysts are those already present on the Mo sample. The role of nickel would be to activate them. This gains some support in view of the suggested structure of the Mo-16–Ni-*y* samples (Fig. 5) which could show a possible analogy with the $Ni(MoS_4)_2^{2-}$ complex of Müller and Diemann (*26*). These heteropolyanions present interesting electrochemical properties, with two reversible reductions centered on the Ni atom (*27*). The high Mo-content Ni–Mo catalysts might catalyze the HDS reaction according to a redox mechanism as proposed by Schuit and Gates (*1*) in which the Ni atoms play an essential role by electron transfer.

Low and High Ni Content in Ni–Mo/Al_2O_3 Catalysts

The occurrence of a Ni_F/Mo_A domain in which the first free nickel ions (0.3×10^{-4} mol g^{-1}) have a weak promoting effect is rather surprising. In fact one would expect that, subtracting the Ni ions lost in the alumina support, an immediate action of the promoter would be observed, as with unsupported MoS_2 (*6*) and carbon-supported catalysts (*28*). Therefore, in the case of our examination of alumina-supported samples, one could think that a small fraction of the nickel spinel is extracted together with the free nickel upon acid attack, leading to an overestimation of the Ni_F fraction. However, this is unlikely since in that case Fig.

2 would show the line for extracted Ni vs total Ni intercepting the abscissa axis much below zero.

Thus the nature of these first Ni ions is not clear. They show similar characteristics to those observed in the intermediate concentration range, but they are unable to promote the activity of the Mo-based catalysts. Some interaction with oxysulfide Mo species, remaining in small amount upon sulfidation, and especially in the case of thiophene sulfiding, cannot be excluded.

Free nickel atoms in the high concentration range, beyond the maximum, are most probably present as bulk sulfide Ni_3S_2. Once the sulfided molybdenum phase has accommodated the amount of promoter in accordance with the available sites, further added nickel acts as it does in Ni/Al_2O_3 catalysts, with a low participation to the catalytic activity. Finally, as shown in Fig. 5, a too large excess of nickel is likely to stack as Ni_3S_2 either mainly on the alumina (Mo-7–Ni-*x*) or on both alumina and the Ni–Mo–S active phase (Mo-16–Ni-*y*). In that latter case, the promoted molybdenum becomes less accessible to the reactants and the HDS activity decreases. This situation occurs particularly for the Mo-16–Ni-4-*T* catalysts calcined at low temperatures.

CONCLUSION

The present investigation shows that sulfided Ni–Mo/Al_2O_3 catalysts behave in a very distinct way from the corresponding Mo/Al_2O_3 and Ni/Al_2O_3 catalysts. In these studies, the complexity of the γ-alumina-supported catalysts has been clarified by considering the free (extractable) nickel, uncombined with the support, and the work reveals three different actions of the free nickel atoms on the molybdenum catalyst according to the promoter concentration.

On Ni–Mo/Al_2O_3 catalysts activated under thiophene, the main promoting effect appears differently according to the molybdenum concentration in the starting Mo/Al_2O_3 catalyst. At low Mo content, it can be related to the formation of a Ni–Mo–S phase of the type described by Topsøe *et al.* (*7–9*) for Co–Mo–S. The active phase is highly dispersed, and presumably consists of equivalent Mo patches with small size, associating at maximum almost two promoter atoms to three Mo atoms. At higher Mo content, the mild thiophene sulfidation is considered to be inefficient in creating the distinct Mo units, thus leading to a different Ni–Mo–S association, in larger patches.

ACKNOWLEDGMENT

This work has received financial support from D.G.R.S.T. (Paris).

REFERENCES

1. Schuit, G. C. A., and Gates, B. C., *AIChe J.* **19,** 417 (1973).
2. Massoth, F. E., *J. Catal.* **36,** 164 (1975).
3. Voorhoeve, R. J. H., and Stuiver, J. C. M., *J. Catal.* **13,** 243 (1971).
4. Farragher, A. L., and Cossee, P., *in* "Proceedings, 5th International Congress on Catalysis, Palm Beach, 1972" (J. W. Hightower, Ed.), p. 1301. North-Holland, Amsterdam, 1973.
5. De Beer, V. H. J., Van Sint Fiet, T. H. M., van der Steen, G. H. A. M., Zwaga, A. C., and Schuit, G. C. A., *J. Catal.* **35,** 297 (1974).
6. Grange, P., and Delmon, B., *J. Less Common Met.* **36,** 353 (1974).
7. Topsøe, H., Clausen, B. S., Candia, R., Wivel, C., and Mørup, S., *J. Catal.* **68,** 433 (1981).
8. Wivel, C., Candia, R., Clausen, B. S., Mørup, S., and Topsøe, H., *J. Catal.* **68,** 453 (1981).
9. Topsøe, H., Clausen, B. S., Candia, R., Wivel, C., and Mørup, S., *Bull. Soc. Chim. Belg.* **90,** 1189 (1981).
10. Wentrcek, P. R., and Wise, H., *J. Catal.* **51,** 80 (1978).
11. Phillips, R. W., and Fote, A. A., *J. Catal.* **41,** 168 (1976).
12. Candia, R., Clausen, B. S., and Topsøe, H., *J. Catal.* **77,** 564 (1982).
13. Topsøe, H., Clausen, B. S., Burriesci, N., Candia, R., and Mørup, S., *in* "Preparation of Catalysts II" (B. Delmon, P. Grange, P. Jacobs, and C. Poncelet, Eds.), p. 479. Elsevier, Amsterdam, 1979.
14. Breysse, M., Bennett, B. A., Chadwick, D., and Vrinat, M., *Bull. Soc. Chim. Belg.* **90,** 1271 (1981).

15. Clausen, B. S., Topsøe, H., Candia, R., Villadsen, J., Lengeler, B., Als-Nielsen, J., and Christensen, F., *J. Phys. Chem.* **85,** 3868 (1981).
16. Topsøe, N. Y., *J. Catal.* **64,** 235 (1980).
17. Topsøe, N. Y., and Topsøe, H., *Bull. Soc. Chim. Belg.* **90,** 1311 (1981).
18. Bachelier, J., Ph.D. thesis, Univ. Caen, France (1982).
19. Bachelier, J., Tilliette, M. J., Duchet, J. C., and Cornet, D., *J. Catal.* **76,** 300 (1982).
20. Bachelier, J., Duchet, J. C., and Cornet, D., *Bull. Soc. Chim. Fr.* **I,** 112 (1978); and **I,** 221 (1979).
21. Bachelier, J., Duchet, J. C., and Cornet, D., *J. Catal.* **87,** 283 (1984).
22. Topsøe, N. Y., and Topsøe, H., *J. Catal.* **77,** 293 (1982).
23. Grimblot, J., Dufresne, P., Gengembre, L., and Bonnelle, J. P., *Bull. Soc. Chim. Belg.* **90,** 1261 (1981).
24. Burch, R., and Collins, A., "Proceedings, 4th International Conference on Chemistry and Uses of Molybdenum," (H. F. Barry and P. C. H. Mitchell, Eds.), p. 397. Climax Molybdenum Company, Ann Arbor, Mich., 1982.
25. Topsøe, H., Invited paper presented at "Advances in Catalytic Chemistry II" Symposium, Salt Lake City, 1982.
26. Müller, A., and Diemann, E., *Chem. Commun.* **65** (1971).
27. Callahan, K. P., and Piliero, P. A., *Inorg. Chem.* **19,** 2619 (1980).
28. Duchet, J. C., van Oers, E. M., de Beer, V. H. J., and Prins, R., *J. Catal.* **80,** 386 (1983).